Journal of Computational Physics **183,** 563–576 (2002)
doi:10.1006/jcph.2002.7209

The Moment Propagation Method for Advection–Diffusion in the Lattice Boltzmann Method: Validation and Péclet Number Limits

R. M. H. Merks, A. G. Hoekstra, and P. M. A. Sloot

Section of Computational Science, University of Amsterdam, Kruislaan 403, 1098 SJ Amsterdam, The Netherlands
E-mail: {roel, alfons, sloot}@science.uva.nl

Received August 13, 2001; revised August 13, 2002

We numerically validate the moment propagation method for advection–diffusion in a lattice Boltzmann simulation against the analytic Taylor–Aris prediction for dispersion in a three-dimensional Poiseuille flow. Good agreement between simulation and theory is found, with relative errors smaller than 2%. The Péclet number limits on the moment propagation method are studied, and maximum parameter values are obtained. We show that a modification of the moment propagation method allows advection–diffusion simulations with higher Péclet numbers, in particular in the low Reynolds number limit.

Key Words: lattice Boltzmann method; moment propagation method; advection–diffusion; Taylor–Aris dispersion.

1. INTRODUCTION

Lattice Boltzmann methods (LBMs) are widely used in fluid dynamics applications as an alternative to numerical solutions of the Navier–Stokes equation [4]. LBMs are well suited for parallel simulation [13] and they are especially useful in problems with obstacles of complex geometry (see, for example, [5, 11, 14, 15]).

In many fluid dynamics applications one is interested in the dispersion of a solute in a fluid. Examples of such advection–diffusion problems are the spreading of contaminants in ground water [2], the transport of heat and water vapour from seed potato packagings [22], tracer dispersion in rough fractures [7], and the transport of nutrients towards a growing coral colony [11].

Apart from numerical solutions of the macroscopic advection–diffusion equation, several methods have been developed to solve advection–diffusion using tracer particle

0021-9991/02 $35.00

distributions. In stochastic methods, discrete particles carry out a random walk that is biased by the velocity field [19]. Mesoscopic advection–diffusion methods use particle densities rather than discrete particles. Examples of such mesoscopic methods are Flekkøy's method [8] and the method of Dawson and co-workers [6, 16]. These methods solve a multiple species miscible flow using the LBM. A similar method is Van der Sman's method [23]. Van der Sman solves a lattice Boltzmann equation for advection–diffusion, in which the collision operator is biased by an externally imposed velocity field. The method of Calí *et al.* uses the fourth velocity component in a four-dimensional flow projected onto a lower dimensional lattice as a tracer [3].

Another mesoscopic method is the moment propagation method [17], which we aim to validate in this paper. In this method a single scalar per site for each tracer species is propagated. The direction of propagation is biased by the velocity field. The moment propagation method was originally developed to efficiently calculate the velocity autocorrelation function (VACF) in lattice gas cellular automata [9, 10, 21] and was later used to calculate the VACF in the lattice Boltzmann method [17, 18]. The moment propagation method has been used to solve the advection–diffusion equation in a simulation of the transport of nutrients to a growing coral colony [11] and was further developed to solve electroviscous transport problems [24].

The moment propagation method has a few advantages relative to other tracer dispersion methods. In many applications one needs a preaveraged, smooth distribution of tracer. For these applications a stochastic method [19] may not be the most efficient. Since the moment propagation method uses only a single scalar per site for each tracer species, the computational and memory requirements are much lower than for the other methods. Also, the addition of extra tracer species is relatively easy. Hence, the moment propagation method seems to be a good choice for solute dispersion applications.

We are unaware of any attempts to numerically validate the moment propagation method against analytic benchmarks. In this paper, we undertake such validation by comparing the moment propagation method against the analytic Taylor–Aris result of solute dispersion in three-dimensional tubes [1].

In addition, we study the Péclet number limits of the moment propagation method. We find a maximum value of the Péclet number beyond which negative solute concentrations occur. We present a modification of the moment propagation method, which allows higher Péclet numbers than the standard moment propagation method.

2. SIMULATION METHODS

2.1. Lattice Boltzmann BGK Method

To obtain the flow field in which the solutes were dispersed, we applied a special form of the lattice Boltzmann method, the lattice Boltzmann BGK (Bhatnager, Gross, Krook) method (denoted hereafter as LBGK) [20]. The lattice Boltzmann equation is solved on a discrete lattice x. On each lattice point there is a set of particle densities f_i of discrete velocity $\vec{c}_i$. For each time step Δt, the density f_i is propagated along the lattice according to its velocity $\vec{c}_i$. The discrete velocities $\vec{c}_i$ are such that in one time step the particle densities stream from one lattice site to a neighbouring lattice site. Next, the particle densities are redistributed according to the collision operator Ω_i. The general form of the lattice

Boltzmann equation is

$$f_i(\vec{x} + \Delta t\vec{c}_i, t + \Delta t) = f_i(\vec{x}, t) + \Omega_i, \tag{1}$$

in which Ω is the collision operator and $\vec{c}_i$ is the velocity of the particle density f_i.

The density ρ and the fluid velocity $\vec{u}$ are obtained from the first- and second-order moments of the particle distributions

$$\rho(\vec{x}, t) = \sum_i f_i(\vec{x}, t) \tag{2}$$

and

$$\vec{u}(\vec{x}, t) = \frac{\sum_i f_i(\vec{x}, t)\vec{c}_i}{\rho(\vec{x}, t)}. \tag{3}$$

We used the D_3Q_{19} model on a cubic lattice. This model is isotropic and satisfies the Navier–Stokes equations [4].

The collision operator Ω_i can take different forms. In the LBGK method [20], the particle distribution f is relaxed towards the equilibrium distribution f^{eq}, through

$$\Omega_i = \frac{1}{\tau}\left(f_i^{\text{eq}}(\vec{x}, t) - f_i(\vec{x}, t)\right). \tag{4}$$

The equilibrium distribution $f^{\text{eq}}(\vec{x}, t)$ is a function of the local density $\rho(\vec{x}, t)$ and the local velocity $\vec{u}(\vec{x}, t)$,

$$f_i^{\text{eq}}(\rho, \vec{u}) = t_p\rho\left(1 + \frac{\vec{c}_i \cdot \vec{u}}{c_s^2} + \frac{(\vec{c}_i \cdot \vec{u})^2}{2c_s^4} - \frac{\vec{u} \cdot \vec{u}}{2c_s^2}\right), \tag{5}$$

in which c_s is the speed of sound, the index $p = \vec{c}_i \cdot \vec{c}_i$ is the square length of the lattice vectors, and t_p is the corresponding equilibrium density for $\vec{u} = 0$ [20]. For the D_3Q_{19} lattice, which we have used in this paper, $t_0 = 1/3$, $t_1 = 1/18$, and $t_2 = 1/36$.

The relaxation parameter τ determines the kinematic viscosity ν of the simulated fluid. For the D_3Q_{19} lattice $\nu = (2\tau - 1)/6$ [4]. Throughout this paper, $\tau = 1.0$ ($\nu = 1/6$). This value for τ is well above the safe lower limit of τ [20]. At solid boundaries, a halfway bounce-back boundary condition was applied [12].

To speed up the computation of a stable flow field, we routinely use the *iterative momentum relaxation* technique [12]. In this technique, a body force is iteratively balanced with the frictional forces of the obstacle. The iterative momentum relaxation is started as soon as the fluid velocity exceeds a desired minimal velocity.

2.2. The Moment Propagation Method

After the iteration of Eq. (1), until a stable flow field $f(\vec{x})$ is obtained, the dispersion of tracers using the moment propagation method [17] is started. In this method, a scalar quantity $P(\vec{x}, t)$ is released in the lattice. A fraction Δ/ρ of $P(\vec{x}, t)$ stays on the lattice node and the remaining fraction is distributed over the neighbouring nodes according to the

probability $f(\vec{x}-\vec{c}_i,t)$ that a carrier fluid particle moves with velocity $\vec{c}_i$ after collision, giving

$$P(\vec{x},t+1)=\sum_i \frac{(f_i(\vec{x}-\vec{c}_i)-\Delta/b)P(\vec{x}-\vec{c}_i,t)}{\rho(\vec{x}-\vec{c}_i)}+\Delta\frac{P(\vec{x},t)}{\rho(\vec{x})}, \tag{6}$$

where b is the number of velocities in the lattice (in our case $b=19$). The parameter Δ is used to set the molecular diffusion coefficient D_m. The dependence of D_m on Δ for a D_3Q_{19} lattice is found as follows. Assuming that the moment propagation method solves the advection–diffusion equation, we can find the diffusion constant by considering the dispersion of tracer after one time step. A δ-pulse of tracer is released in a flow field in equilibrium at $t=0$. At $t=1$, the first- and second-order moments $\vec{m}_1$ and m_2 are

$$\vec{m}_1=\sum_i \frac{f_i^{\mathrm{eq}}(\vec{u},\rho)-\frac{\Delta}{19}}{\rho}\vec{c}_i=\vec{u} \tag{7}$$

and

$$m_2=\sum_i \frac{f_i^{\mathrm{eq}}(\vec{u},\rho)-\frac{\Delta}{19}}{\rho}\vec{c}_i\cdot\vec{c}_i=1+\vec{u}\cdot\vec{u}-\frac{30}{19}\frac{\Delta}{\rho}. \tag{8}$$

Using $D_m=\frac{1}{6}\frac{d(m_2-\vec{m}_1\cdot\vec{m}_1)}{dt}=\frac{1}{6}[m_2-\vec{m}_1\cdot\vec{m}_1]_{t=1}$, we find that

$$D_m=\frac{1}{6}-\frac{5}{19}\frac{\Delta}{\rho}. \tag{9}$$

We measured D_m in a D_3Q_{19} model for a wide range of values of Δ. These measurements agreed with Eq. (9), with a residual sum of squares of 4×10^{-17} (data not shown).

The diffusion coefficient can also be derived from the moment propagation method without the prior assumption that it solves the advection–diffusion equation. Following the method used by Warren [24], where a uniform flow field is assumed, it is straightforward to show that the moment propagation method (Eq. (6)) approximates to second order the advection–diffusion equation

$$\frac{\partial P}{\partial t}+\vec{u}\cdot\mathrm{grad}\,P=D_m\nabla^2P. \tag{10}$$

For the diffusion coefficient D_m, this analysis results in the expression

$$D_m=\frac{1}{2}\left(c_s^2-\frac{1}{bd}\sum_i\vec{c}_i\cdot\vec{c}_i\frac{\Delta}{\rho}\right), \tag{11}$$

with b the number of velocities in the lattice and d the dimensionality of the lattice. Note that for the D_3Q_{19} lattice, for which $c_s=1/\sqrt{3}$ [20], this equation agrees with the result obtained in Eq. (9).

At solid boundaries, a halfway bounce-back boundary condition was used; tracer that is propagated into a solid point bounces back immediately and stays where it was.

3. RESULTS

3.1. Taylor–Aris Dispersion in 3D Poiseuille Flow

The moment propagation (MP) method was validated against the analytic Taylor–Aris prediction of tracer dispersion in a fluid flowing through a straight cylindrical tube [1]. In this theory, the dispersion coefficient K describes the dispersion of tracer about a point moving with the mean flow velocity $\bar{u}$; $K = \frac{1}{2}\frac{\partial(\sigma_{xx}^2 - (\sigma_x)^2)}{\partial t}$, where σ_x and σ_{xx}^2 are the first- and second-order moments of the spatial tracer distribution along the flow direction. Aris has shown that the dispersion coefficient K is the sum of the molecular diffusion coefficient D_m and of a contribution by advection,

$$K = D_m + \kappa\alpha^2\bar{u}^2/D_m, \tag{12}$$

where, in the case of a three-dimensional Poiseuille flow, $\kappa = 1/48$ and α is the tube radius.

The simulations were carried out in a simulation box with a cross section of 54×54 lattice units, in which a tube of radius 25 was constructed. We initiated the simulation with a δ-pulse of solute in the middle of the tube. The first- and second-order moments parallel to the flow direction σ_x and σ_{xx}^2 were measured, from which the spatial variance $V = \sigma_{xx}^2 - (\sigma_x)^2$ was computed. After an initial transient, approximately the time needed for the solute to reach the wall of the tube by diffusion, the tracer variance V increased linearly with a slope of $2K$. This linear dependence no longer holds when a fraction of tracer reaches the end of the tube and reenters the tube over the periodic boundary. This time of reentry is dictated by advection and diffusion along the flow direction.

The size of the simulation box was set by considering estimations of the length of the initial transient and of the tracer reentry time. In this way it was ensured that the two time scales did not overlap, enabling the observation of the linear domain, which was needed for measuring the dispersion coefficient. The length of the initial transient was estimated as follows. The initial pulse of solute diffuses perpendicularly to the flow direction as a Gaussian. Using $t_D = \frac{r^2}{2D_m}$, for the range of diffusion constants considered, the time t_D at which 66% of the tracer has reached the walls of the tube is in the range $1750 < t_D < 3500$. The tracer reentry time depends on the length of the tube. The time needed for 1% of solute in a fluid moving at a uniform velocity $u_{\max}$ to travel a distance Δx by means of diffusion and advection was estimated by solving the equation $ut + 3\sqrt{2D_m t} = \Delta x$. Hence, the settings of the simulation box length were based on the mean velocity and on the diffusion coefficient (see Table I), thus compromising between tracer reentry times and computational resources.

TABLE I
Settings of the Simulation Box Length

D_m	$\bar{u}$	Tube length
<0.1	$\bar{u} \le 0.01$	800
<0.1	$0.02 \le \bar{u} \le 0.04$	1600
<0.1	$0.04 \le \bar{u} \le 0.07$	3200
<0.1	$\bar{u} \ge 0.07$	6400
0.166	$\bar{u} < 0.03$	800
0.166	$0.01 \le \bar{u} \le 0.03$	1600
0.166	$0.03 \le \bar{u} \le 0.05$	3200
0.166	$\bar{u} \ge 0.05$	6400

A stable (paraboloid) flow field was computed for a range of mean flow velocities between 0.0 and 0.103 in lattice units per time step. For a 3D Poiseuille flow, the maximum velocity $u_{\max} = 2\bar{u}$, giving a maximum flow velocity of 0.206. These flow velocities correspond to Reynolds numbers ($Re = \frac{\bar{u}l}{\nu}$, where $l = 25$ l.u., the tube radius) between 0.0 and 15.5, which are all in the laminar regime. We measured the lattice Péclet number $\text{Pé}_{\text{lat}} = \frac{u_{\max} l}{D_m}$, in which $l = 1$ l.u. The lattice Péclet number is locally defined with respect to the lattice nodes of the advection–diffusion simulation and is independent of the size of the obstacle. The maximum lattice Péclet numbers occurring in the simulations were between 0.0 ($u_{\max} = 0$, $D_m = 1/6$) and 1.892 ($u_{\max} = 2\bar{u}_{\max} = 0.182$, $D_m = 0.096$).

In Fig. 1 we have plotted the time-dependent dispersion coefficient $D(t) = \frac{1}{2}\frac{dV(t)}{dt}$. At $t = 0$, the dispersion coefficient was equal to the molecular diffusion coefficient $D(0) = D_m$. As the initial delta pulse spread in the y- and z-directions by diffusion, the dispersion coefficient increased until it reached the Taylor–Aris prediction (the dotted lines). It is easy to see that the dispersion coefficient should increase as the delta pulse spreads over the paraboloid flow field; the initial field of solute expands ever more quickly as tracer diffuses into layers of lower velocity and lags behind the tracer moving in flow layers of higher velocity. The duration of the initial transient t_D was somewhat shorter than our estimation earlier in this section. This shows that it was a conservative assumption that 66% of the tracer should have reached the tube wall for the initial transient to end.

We measured the dispersion coefficient D in a time window well after our estimate of the initial transient and well before the estimation of the onset of tracer reentry. The dispersion coefficients were plotted together with the prediction according to the Taylor–Aris theory in Fig. 2. All simulated values were within a 2% range from the analytical Taylor–Aris result. Hence, our simulation results are in good agreement with the Taylor–Aris theory.

3.2. Limits to the Péclet Number

In the moment propagation method (Eq. (6)) the diffusion coefficient is set using parameter Δ, which is the probability that a tracer particle stays at the same lattice site. This poses a limit onto the maximum Péclet number that can be simulated using the MP method. The reason is that negative tracer concentrations may appear if the value $f_i(\vec{x}_i - c_i) - \frac{\Delta}{b}$ in Eq. (6) becomes negative. In this section we investigate the maximum Péclet number that can be used in an MP simulation to ensure that $\forall_{\vec{x},i} : \frac{\Delta}{b} \leq f_i(\vec{x})$.

The maximum lattice Péclet number follows from the maximum Δ for which each streamed tracer quantity $f_i(\vec{x} - c_i) - \Delta/b \geq 0$ (see Eq. (6)). Assuming to first approximation that $f_i \approx f_i^{\text{eq}}$, we can write ($f_{\min} = \min(f_i)$),

$$\Delta_{\max}(\rho, \vec{u}) = b f_{\min}^{\text{eq}}(\vec{u}_{\max}, \rho), \tag{13}$$

in which $b = 19$ for the D_3Q_{19} model and f^{eq} is the equilibrium distribution (Eq. (5)). The maximum lattice Péclet number is calculated using the diffusion coefficient (Eq. (9)), giving

$$\text{Pé}_{\max} = \frac{|\vec{u}_{\max}|}{D_{\min}} = \frac{|\vec{u}_{\max}|}{\frac{1}{6} - 5 f_{\min}^{\text{eq}}(\vec{u}_{\max}, \rho)}, \tag{14}$$

in which $|\vec{u}_{\max}|$ is the maximum velocity occurring in the simulation.

In Fig. 3 we have plotted the maximum lattice Péclet number for which the MP method still gives valid results. The maximum allowed lattice Péclet number is plotted for three

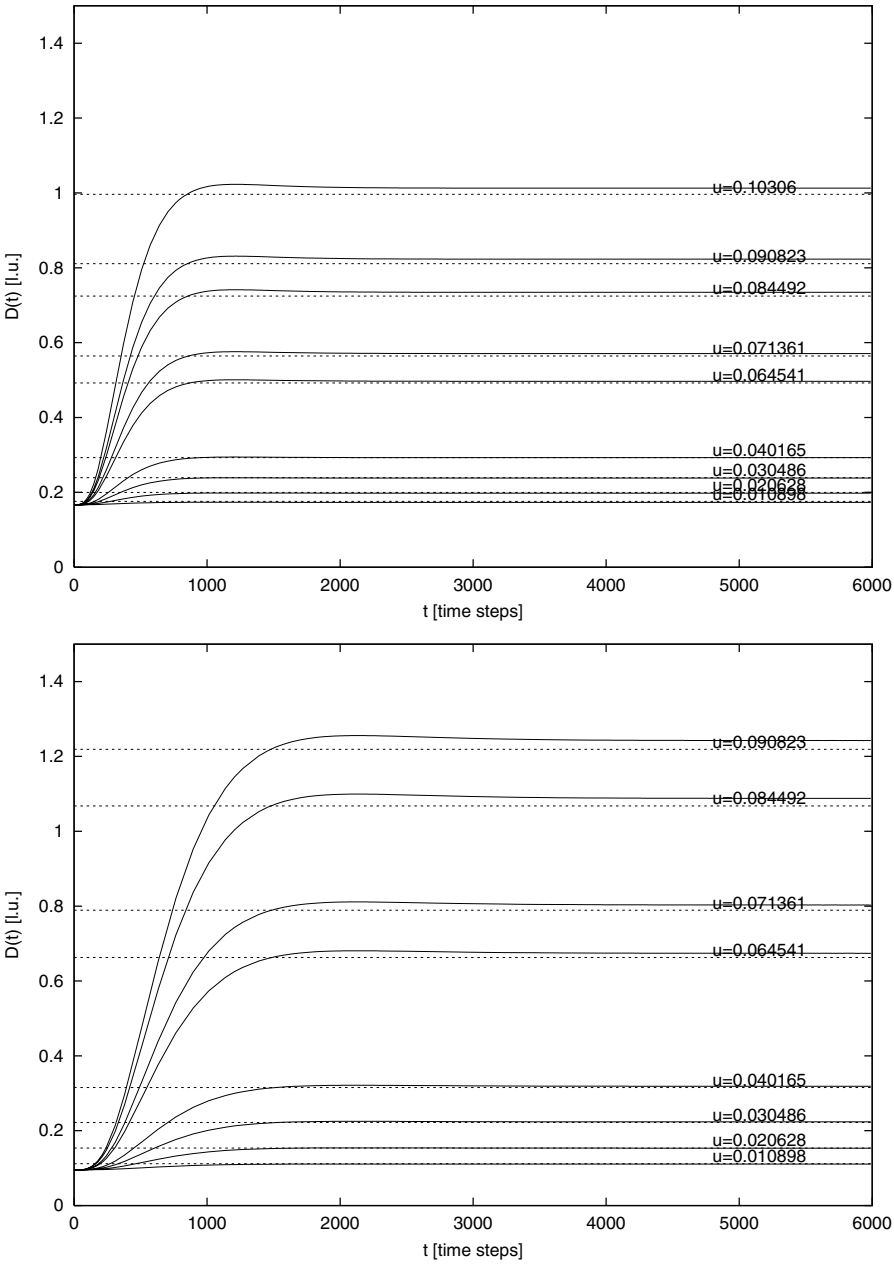

FIG. 1. Validation of the moment propagation scheme. The time-dependent dispersion coefficients $D(t) = \frac{1}{2}\frac{dV(t)}{dt}$, in which $V = \sigma_{xx}^2 - (\sigma_x)^2$, were measured in a 3D Poiseuille flow in a tube of radius 25. $\Delta = 0$ ($D_m = 1/6$) and $\Delta = 0.27$ ($D_m = 0.096$) for the upper and lower panels, respectively. The tube lengths were set according to Table I. The mean flow velocity $u = \frac{1}{2}u_{\max}$ is given for each line in lattice units. The Taylor–Aris predictions of the dispersion coefficients are shown as dashed lines.

flow directions. Of these three flow directions, the direction (1,1,0) gives the lowest allowed Péclet number. For this flow direction the smallest possible value of f_i will occur opposite the dominating flow direction. In the D_3Q_{19} model, the velocities $|\vec{c}_i| = \sqrt{2}$ will generally have the lowest density f_i. For these velocities $t_p = 1/36$ (see Eq. (5)).

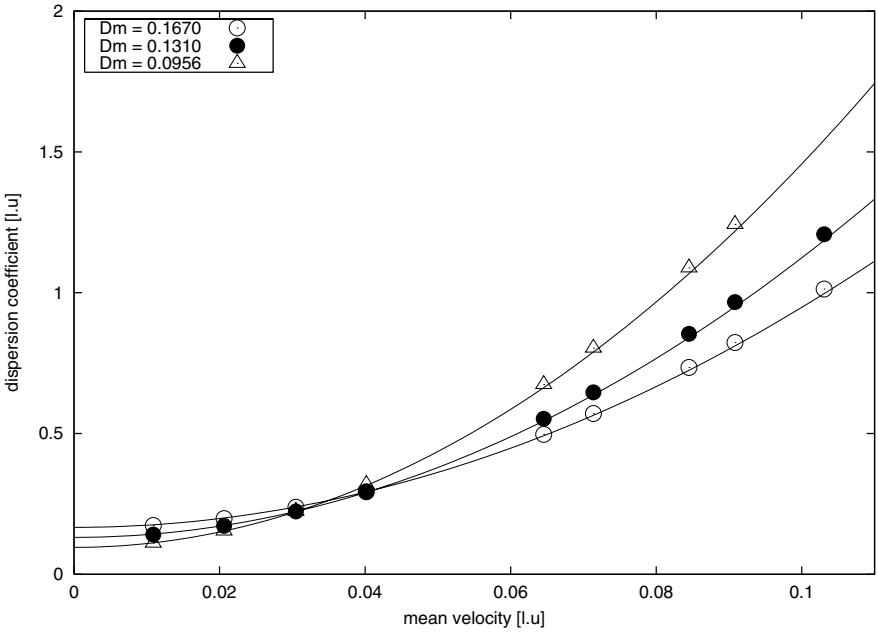

FIG. 2. Dispersion coefficients computed with the moment propagation method for a three-dimensional Poiseuille flow in a cylindrical tube of radius 25. The Taylor–Aris prediction is shown as a solid line. The length of the tube was varied between 800 and 6400 l.u., depending on the flow velocity and the diffusion coefficient. See text for further details. All simulated values were within a 2% interval from the prediction.

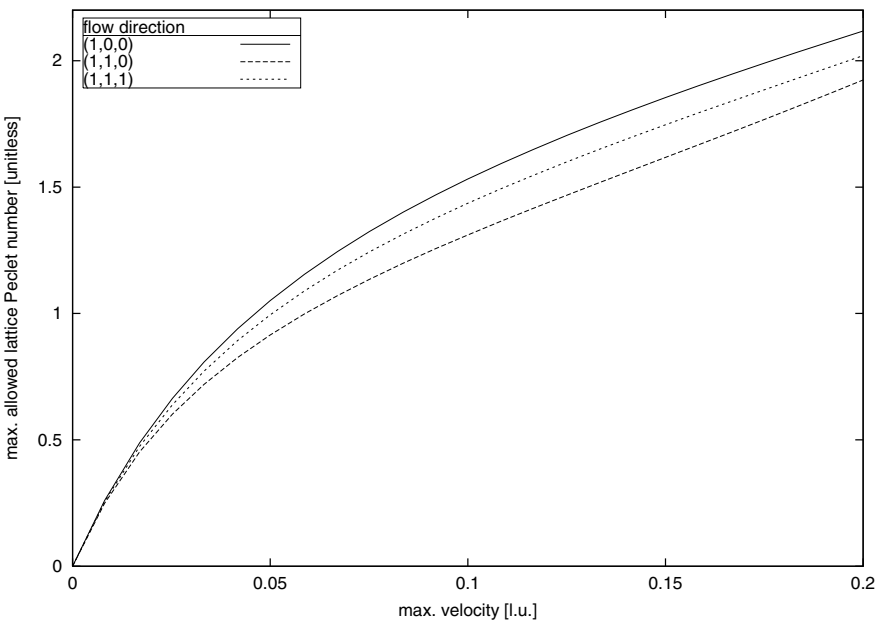

FIG. 3. The maximum lattice Péclet numbers that can be simulated using the moment propagation method and the LBGK method on a D_3Q_{19} lattice is plotted against the norm of the maximum velocity occurring in the simulation. Velocities directed along the two lattice vectors (1,0,0) and (1,1,0) and along the nonlattice vector (1,1,1) are shown. The use of lattice Péclet numbers higher than the maximum allowed Péclet number may result in negative tracer concentrations.

3.3. A Modification of the Moment Propagation Method

In the standard MP scheme, the molecular diffusion coefficient D_m is lowered by subtracting an equal amount of tracer Δ/b from the tracer moving to the neighbouring sites. As we argued in Section 3.2, this may lead to negative tracer values, especially for the relatively small values of f_i for the velocities $|\vec{c}_i| = \sqrt{2}$.

This problem can be diminished by using the following modification of the moment propagation method. In this modified scheme, the amount of resting tracer particles is weighted according to the equilibrium distribution for a resting fluid $f_i^{\mathrm{eq}}(u = 0, \rho)$,

$$P(\vec{x}, t+1) = \sum_i \left[\frac{(f_i - \Delta^* f_i^{\mathrm{eq}}(\vec{u} = 0, \rho))P}{\rho} \right]_{\vec{x}-\vec{c}_i, t} + \Delta^* P(\vec{x}, t), \tag{15}$$

where the whole quantity inside [. . .] is evaluated at $(\vec{x} - \vec{c}_i, t)$. Hence, we adjust the amount of extra rest particles in the streaming direction. The dimensionless parameter Δ^* is the fraction of tracer remaining at the same lattice site after propagation. Note from Eq. (5) that $f_i^{\mathrm{eq}}(\vec{u} = 0, \rho) = t_p \rho$, so we can rewrite Eq. (15) as

$$P(\vec{x}, t+1) = \sum_i \left[\left(\frac{f_i}{\rho} - t_p \Delta^* \right) P \right]_{\vec{x}-\vec{c}_i, t} + \Delta^* P(\vec{x}, t), \tag{16}$$

which is equivalent to the moment propagation method introduced by Warren [24].

The molecular diffusion coefficient D_m is set using parameter Δ^*, as in the standard MP scheme. Releasing a δ-pulse, after one time step the first- and second-order moments $\vec{m}_1$ and m_2 are

$$\vec{m}_1 = \sum_i \frac{f_i^{\mathrm{eq}}(\vec{u}, \rho) - \Delta^* f_i^{\mathrm{eq}}(\vec{u} = 0, \rho)}{\rho} \vec{c}_i = \vec{u} \tag{17}$$

and

$$m_2 = \sum_i \frac{f_i^{\mathrm{eq}}(\vec{u}, \rho) - \Delta^* f_i^{\mathrm{eq}}(\vec{u} = 0, \rho)}{\rho} \vec{c}_i \cdot \vec{c}_i = 1 + \vec{u} \cdot \vec{u} - \Delta^*. \tag{18}$$

Thus, the diffusion coefficient $D_m = \frac{1}{6} \frac{d(m_2 - \vec{m}_1 \cdot \vec{m}_1)}{dt} = \frac{1}{6}[m_2 - \vec{m}_1 \cdot \vec{m}_1]_{t=1}$ depends on Δ^* as

$$D_m = \frac{1}{6} - \frac{1}{6}\Delta^*. \tag{19}$$

Our measurements agreed with this expression, with a residual sum of squares of 1×10^{-16} (data not shown). Warren has shown analytically for a uniform flow field that this scheme approximates to second order the advection–diffusion equation (Eq. (10)) with $D_m = \frac{1}{2} c_s^2 (1 - \Delta^*)$. Note that this expression for the diffusion coefficient agrees with Eq. (19).

Using the reformulation of the MP scheme, we can reach higher Péclet numbers without obtaining negative tracer concentrations. As in Section 3.2, the Péclet number limits of the modified moment propagation scheme (MMP scheme) are calculated from the maximum allowed Δ^*, $\Delta^*_{\max}(\vec{u})$, which can be obtained from Eq. (15):

$$\Delta^*_{\max}(\vec{u}) = \min \left(\frac{f_i^{\mathrm{eq}}(\vec{u}, \rho)}{f_i^{\mathrm{eq}}(\vec{u} = 0, \rho)} \right). \tag{20}$$

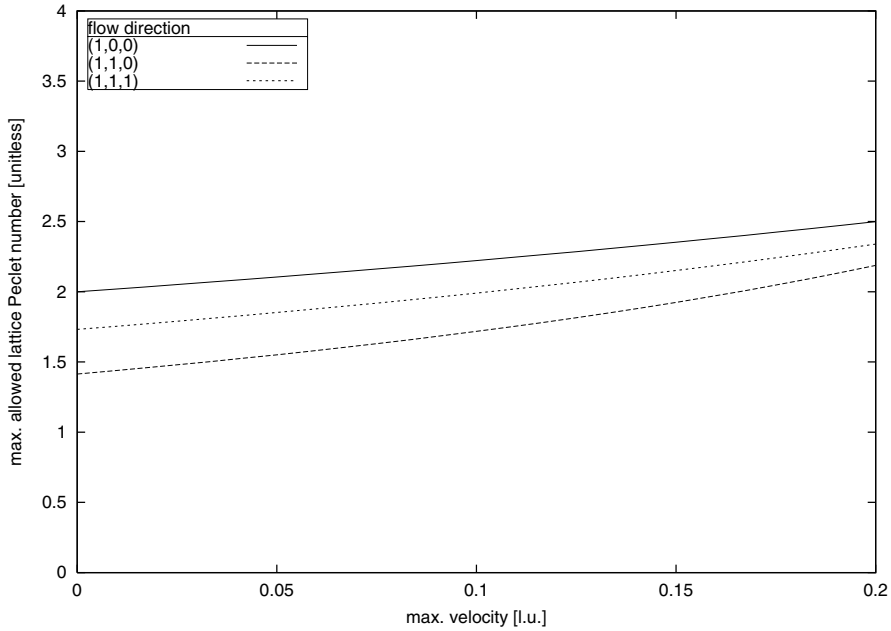

FIG. 4. The maximum lattice Péclet numbers that can be simulated using the modified moment propagation method and the LBGK method on a D_3Q_{19} lattice. Velocities directed along the two lattice vectors (1,0,0) and (1,1,0) and along the nonlattice vector (1,1,1) are shown. The use of lattice Péclet numbers higher than the maximum allowed Péclet number may result in negative tracer concentrations.

The maximum allowed lattice Péclet number follows from Eqs. (19) and (20):

$$\mathrm{Pé}_{\max}(\vec{u}_{\max}) = \frac{|\vec{u}_{\max}|}{D_{\min}} = \frac{|\vec{u}_{\max}|}{\frac{1}{6} - \frac{1}{6}\Delta^*_{\max}(\vec{u}_{\max})}. \tag{21}$$

In Fig. 4 the maximum allowed lattice Péclet number in the MMP scheme is plotted against the maximum velocity occurring in the simulation.

For typical velocities of 0.05 to 0.1 l.u., the maximum Péclet number in the MMP scheme is 1.7 to 1.3 times higher than in the MP scheme. For lattice velocities in the limit to 0, the maximum lattice Péclet number is still at least $\sqrt{2}$ for the MMP scheme, whereas in the MP scheme the maximum lattice Péclet number approaches 0. From Eq. (20) it follows that for the MMP scheme $\lim_{u\to 0} \Delta^*_{\max} = 1$, so $(D_m)_{\min} = 0$. This means that in the low lattice velocity limit, the normal operation limit of the LBGK method, one can still set the diffusion coefficient small enough to reach Péclet numbers up to $\sqrt{2}$. In the MP scheme however, $\lim_{u\to 0} \Delta_{\max} = 19 f^{\mathrm{eq}}_{\min}(\vec{u} = 0, \rho) = \frac{19\rho}{36}$, giving $(D_m)_{\min} = 1/36$. So, in the low lattice velocity limit, in the MP method one cannot set D_m small enough to reach high Péclet numbers.

3.4. Validation of the Modified Moment Progagation Method

We also validated the MMP scheme against the Taylor–Aris prediction of dispersion in a three-dimensional Poiseuille flow. We set $\Delta^* = 0.50$, for which $D_m = 0.083$. This value of Δ^* is very close to the maximum allowed Δ^* for $u_{\max} = 0.2$ ($\Delta^*_{\max} = 0.52$). The tube lengths were set according to the data in Table I.

In Fig. 5 the time-dependent dispersion coefficient $D(t)$ is plotted. After the initial transient, the dispersion coefficients approached the Taylor–Aris prediction. In Fig. 6 we have

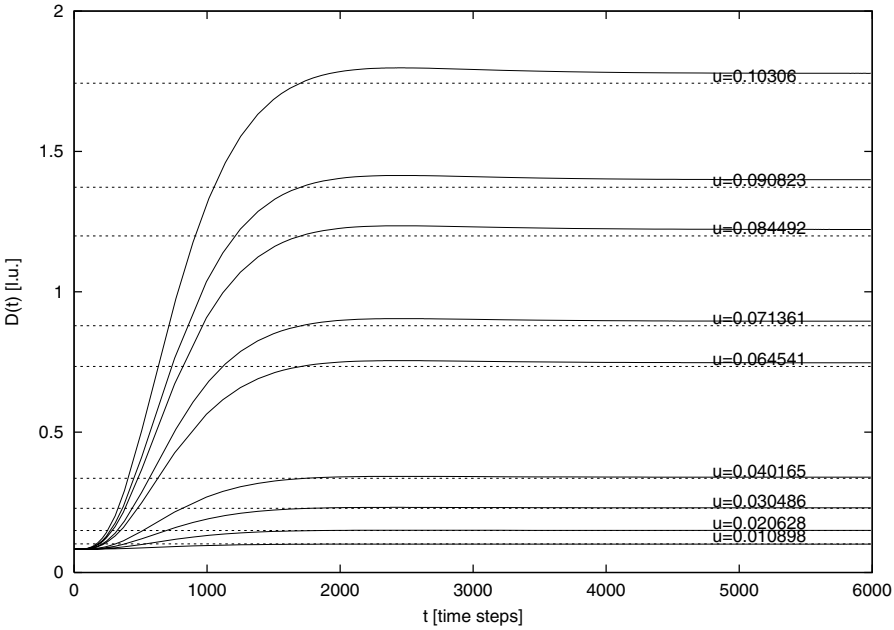

FIG. 5. Validation of the modified moment propagation method. The time-dependent dispersion coefficient $D(t) = \frac{1}{2}\frac{dV(t)}{dt}$, in which $V = \sigma_{xx}^2 - (\sigma_x)^2$, was measured in a 3D Poiseuille flow in a tube of radius 25. $\Delta^* = 0.50$, for which $D_m = 0.083$. The tube length was set according to Table I. The flow velocity in lattice units is given for each line. The Taylor–Aris predictions of the dispersion coefficients are shown as dashed lines.

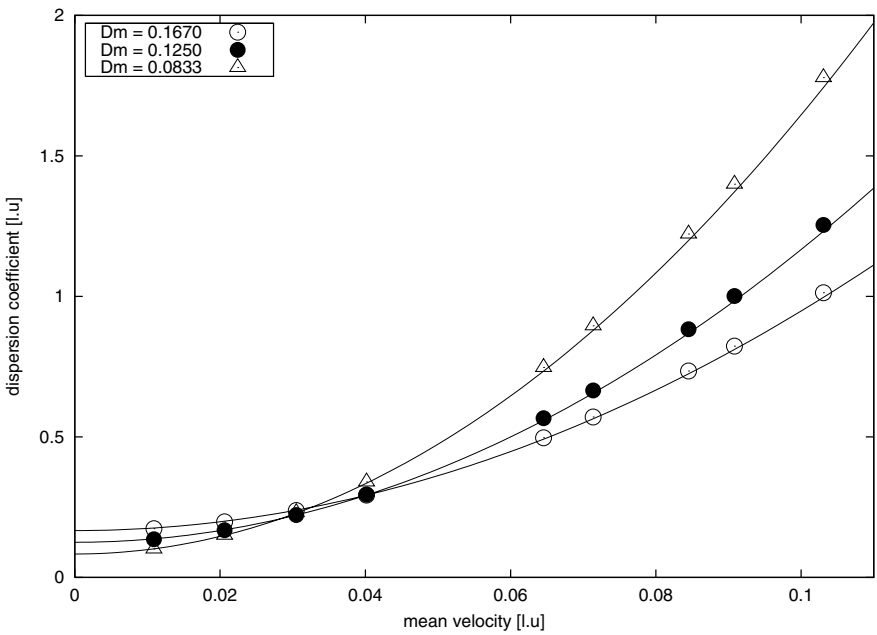

FIG. 6. Dispersion coefficients computed with the modified moment propagation method for a three-dimensional Poiseuille flow in a cylindrical tube of radius 25. The Taylor–Aris prediction is shown as a solid line. Mean flow speeds are given in lattice units. The length of the tube was varied between 800 and 6400 l.u., depending on the flow velocity and the diffusion coefficient. See text for further details. All experimental values were within a 2% interval from the prediction.

plotted the measured Taylor–Aris dispersion coefficients for $D_m = 0.083$, for $D_m = 0.1250$, and for $D_m = 1/6$, together with the Taylor–Aris prediction. Note that for $D_m = 1/6$, there is no difference between the MP and the MMP schemes. All our measurements were less than 2% above the Taylor–Aris prediction.

4. DISCUSSION

In summary, our simulations of dispersion in a three-dimensional Poiseille flow, using the moment propagation method in the LBGK method, reproduced the analytical Taylor–Aris result [1].

For the three-dimensional tube flows, the measured dispersion coefficients were never further than 2% from the Taylor–Aris prediction. The same experiments were carried out for a 2D Poiseuille flow in tubes of width 50 and of 100 l.u. (data not shown). In these experiments, all dispersion coefficients were closer than 1% to the Taylor–Aris prediction. The fact that we still found accurate agreement with the Taylor–Aris prediction in narrow, coarsely discretised circular tubes suggests that the moment propagation method is a suitable method for advection–diffusion problems in complex geometries, such as the transport of nutrients and other chemicals towards a growing coral colony [11].

The dispersion coefficients as obtained in our three-dimensional simulations were systematically slightly larger than the Taylor–Aris predicition. In our two-dimensional simulations the dispersion coefficients approached the Taylor–Aris prediction from below (data not shown). This observation agrees with the findings by Calí *et al.* [3]. Using their method in a two-dimensional Poiseuille flow, they also found dispersion coefficients that were systematically slightly smaller than the Taylor–Aris prediction. These authors attributed their systematic error "to the fact that the assumption on which [the Taylor–Aris prediction] is based is less and less valid as the Péclet-number increases" [3]. Indeed the systematic errors in our two- and three-dimensional simulations increased with the flow velocity.

Note that our simulations also agreed with the Taylor–Aris prediction for values of Δ and Δ^* for which negative concentrations occur (data not shown). Also, measurements of the diffusion coefficient D_m agreed with the predictions in Eqs. (9) and (19) far beyond the maximum values of Δ and Δ^*. However, such parameter values give unphysical results because some tracer concentrations will be negative. It is therefore important to check whether negative concentrations occur in a simulation using the moment propagation method.

Using the modification of the moment propagation method shown in this paper, higher Péclet numbers can be reached than in the standard moment propagation method. As we have shown in Section 3.3, this holds in particular in the low lattice velocity limit, for which the LBM produces more accurate flow fields [4]. To reach the maximum Péclet and Reynolds numbers that are correctly simulated with the moment propagation method, the lattice velocity should be kept at moderate values (<0.1 l.u.), the diffusion coefficient should be set to the minimum value still allowed by Eq. (20), and the kinematic viscosity must be set to a minimal value. In steady-state flows the Péclet number limits are independent of the kinematic viscosity. However, in unsteady flows the assumption that $f_i \approx f_i^{\mathrm{eq}}$ may not always be valid and the Pèclet number limits may consequently be lower.

The moment propagation method has some advantages in comparison to other mesoscopic methods. The memory requirements are low; for each tracer species we need a single scalar per lattice node. By comparison, for most of the other mesoscopic methods (Flekkøy [8],

Dawson *et al.* [6], and Van Der Sman [23]), we would need 19 extra scalars per lattice node for each tracer species in the D_3Q_{19} model. On the machine we use (a Linux Beowulf cluster, on which a `double` is eight bytes long), for a typical lattice of 256^3 we need 2 Gb memory for the flow field and only an extra 128 Mb of memory per tracer species for the moment propagation method. For the other mesoscopic methods we would have needed an extra 2 Gb per tracer species. The method of Calí *et al.* [3] does not need extra memory for the tracer, because it uses a quantity in the flow field itself as a tracer. However, in Calí's method it is not possible to tune the molecular diffusion constant D_m as in the moment propagation method. Also, no extra tracer species can be added, which is a straightforward operation in the moment propagation method.

In summary, in the range of Péclet and Reynolds numbers studied, our simulations of the moment propagation method accurately reproduced the Taylor–Aris prediction of the dispersion coefficient. We found limits to the Péclet numbers, beyond which the moment propagation method produces unphysical results. If these limits to the Péclet number are taken into account, the moment propagation method is a valuable and valid computational tool for the simulation of advection–diffusion processes.

REFERENCES

1. R. Aris, On the dispersion of a solute in a fluid through a tube, *Proc. R. Soc. London Ser. A* **235**, 67 (1956).
2. P. B. Bedient, H. S. Rifai, and C. J. Newell, *Ground Water Contamination, Transport and Remediation* (Prentice Hall PTR, Englewood Cliffs, NJ, 1993).
3. A. Calí, S. Succi, A. Cancelliere, R. Benzi, and M. Gramignani, Diffusion and hydrodynamic dispersion with the lattice Boltzmann method, *Phys. Rev. A* **45**, 5771 (1992).
4. S. Chen and G. D. Doolen, Lattice Boltzmann method for fluid flows, *Annu. Rev. Fluid Mech.* **30**, 329 (1998).
5. D. S. Clague, B. D. Kandhai, R. Zhang, and P. M. A. Sloot, Hydraulic permeability of (un)bounded fibrous media using the lattice Boltzmann method, *Phys. Rev. E* **61**, 616 (2000).
6. S. P. Dawson, S. Chen, and G. D. Doolen, Lattice Boltzmann computations for reaction-diffusion equations, *J. Chem. Phys.* **98**, 1514 (1993).
7. G. Drazer and J. Koplik, Tracer dispersion in two-dimensional rough fractures, *Phys. Rev. E* **63**, 056104 (2001).
8. E. G. Flekkøy, Lattice Bhatnagar-Gross-Krook models for miscible fluids, *Phys. Rev. E* **47**, 4247 (1993).
9. D. Frenkel, Long-time decay of velocity autocorrelation function of two-dimensional lattice gas cellular automata, *Proc. Phys.* **46**, 144 (1989).
10. D. Frenkel and M. H. Ernst, Simulation of diffusion in a two-dimensional lattice-gas cellular automaton—a test of mode-coupling theory, *Phys. Rev. Lett.* **63**, 2165 (1989).
11. J. A. Kaandorp, C. P. Lowe, D. Frenkel, and P. M. A. Sloot, Effect of nutrient diffusion and flow on coral morphology, *Phys. Rev. Lett.* **77**, 2328 (1996).
12. D. Kandhai, A. Koponen, A. Hoekstra, M. Kataja, J. Timonen, and P. M. A. Sloot, Implementation aspects of 3D lattice-BGK: Boundaries accuracy and a new fast relaxation method, *J. Comput. Phys.* **150**, 482 (1999).
13. D. Kandhai, A. Koponen, A. G. Hoekstra, M. Kataja, J. Timonen, and P. M. A. Sloot, Lattice-Boltzmann hydrodynamics on parallel systems, *Comput. Phys. Commun.* **111**, 14 (1998).
14. D. Kandhai, D. J. E. Vidal, A. G. Hoekstra, H. Hoefsloot, P. Iedema, and P. M. A. Sloot, A comparison between lattice-Boltzmann and finite-element simulations of fluid flow in static mixer reactors, *Int. J. Mod. Phys. C* **9**, 1123 (1998).
15. A. Koponen, D. Kandhai, E. Hellen, M. Alava, A. Hoekstra, M. Kataja, K. Niskanen, P. Sloot, and J. Timonen, Permeability of three-dimensional random fiber webs, *Phys. Rev. Lett.* **80**, 716 (1998).
16. R. Kumar, S. S. Nivarthi, H. T. Davis, D. M. Kroll, and R. S. Maier, Application of the lattice-Boltzmann method to study flow and dispersion in channels with and without expansion and contraction geometry, *Int. J. Numer. Methods Fluids* **31**, 801 (1999).

17. C. P. Lowe and D. Frenkel, The super long-time decay of velocity fluctuations in a two-dimensional fluid, *Physica A* **220**, 251 (1995).
18. C. P. Lowe and D. Frenkel, Do hydrodynamic dispersion coefficients exist? *Phys. Rev. Lett.* **77**, 4552 (1996).
19. R. S. Maier, D. M. Kroll, H. T. Davis, and R. S. Bernard, Pore-scale flow and dispersion, *Int. J. Mod. Phys. C* **9**, 1523 (1998).
20. Y. H. Qian, D. D'Humières, and P. Lallemand, Lattice BGK models for Navier-Stokes equation, *Europhys. Lett.* **17**, 479 (1992).
21. M. A. Van der Hoef and D. Frenkel, Long-time tails of the velocity autocorrelation function in 2-dimensional and 3-dimensional lattice-gas cellular automata—a test of mode-coupling theory, *Phys. Rev. A* **41**, 4277 (1990).
22. R. G. M. Van der Sman, Solving the vent hole design problem for seed potato packagings, with the lattice Boltzmann scheme, *Int. J. Comput. Fluid Dyn.* **11**, 237 (1999).
23. R. G. M. van der Sman and M. H. Ernst, Convection-diffusion lattice Boltzmann scheme for irregular lattices, *J. Comput. Phys.* **160**, 766 (2000).
24. P. B. Warren, Electroviscous transport problems via lattice-Boltzmann, *Int. J. Mod. Phys. C* **8**, 889 (1997).